Evaluation of an Atmosphere Revitalization Subsystem for Deep Space Exploration Missions

Jay L. Perry[1], Morgan B. Abney[2], Ruth E. Conrad[3], Kenneth R. Frederick[4], Zachary W. Greenwood[5], Matthew J. Kayatin[6], James C. Knox[7], Robert L. Newton[8], Keith J. Parrish[9], and Kevin C. Takada[10]
NASA, George C. Marshall Space Flight Center, Huntsville, Alabama, 35812, USA

Lee A. Miller[11] and Joseph P. Scott[12]
Jacobs Engineering, Huntsville, Alabama

and

Christine M. Stanley[13]
Qualis Corp., Huntsville, Alabama

An Atmosphere Revitalization Subsystem (ARS) suitable for deployment aboard deep space exploration mission vehicles has been developed and functionally demonstrated. This modified ARS process design architecture was derived from the International Space Station's (ISS) basic ARS. Primary functions considered in the architecture include trace contaminant control, carbon dioxide removal, carbon dioxide reduction, and oxygen generation. Candidate environmental monitoring instruments were also evaluated. The process architecture rearranges unit operations and employs equipment operational changes to reduce mass, simplify, and improve the functional performance for trace contaminant control, carbon dioxide removal, and oxygen generation. Results from integrated functional demonstration are summarized and compared to the performance observed during previous testing conducted on an ISS-like subsystem architecture and a similarly evolved process architecture. Considerations for further subsystem architecture and process technology development are discussed.

Nomenclature

ACFB	=	adsorbent cartridge fixed bed
AES	=	Advanced Exploration Systems
AR	=	atmosphere revitalization
ARREM	=	Atmosphere Resource Recovery and Environmental Monitoring
CDRA	=	carbon dioxide removal assembly
CMA	=	carbon dioxide management assembly

[1] Lead Aerospace Engineer, Space Systems Dept., NASA-MSFC/ES62.
[2] Lead Aerospace Engineer, Space Systems Dept., NASA-MSFC/ES62.
[3] Flight Systems Safety Engineer, Space Systems Dept., NASA-MSFC/QD22.
[4] Test Engineer, Space Systems Dept., NASA-MSFC/ES62.
[5] Aerospace Engineer, Space Systems Dept., NASA-MSFC/ES62.
[6] Aerospace Engineer, Space Systems Dept., NASA-MSFC/ES62.
[7] Aerospace Engineer, Space Systems Dept., NASA-MSFC/ES62.
[8] Chemist, Space Systems Dept., NASA-MSFC/ES62.
[9] Test Director, Space Systems Dept., NASA-MSFC/ES62.
[10] Aerospace Engineer, Space Systems Dept., NASA-MSFC/ES62.
[11] ECLSS Engineer, Jacobs Engineer ESSSA Group, NASA-MSFC/ES62.
[12] ECLSS Chemist, Jacobs Engineer ESSSA Group, NASA-MSFC/ES62.
[13] ECLSS Engineer, Qualis Corp. ESSSA Group, NASA-MSFC/ES62.

EChamber= Environmental Control Chamber
ECLS = environmental control and life support
FTIR = Fourier transform infrared
GC = gas chromatograph
ISS = International Space Station
LfFB = low-flow fixed bed
M-COA = Microlith® catalytic oxidizer assembly
MSD = mass-specific detector
OGA = oxygen generation assembly
PACRATS = Payloads and Components Real-time Automated Test System
PID = proportional-integral-derivative
R2FD = Resource recovery functional demonstration
SDU = Sabatier development unit
SMAC = spacecraft maximum allowable concentration
TCC = trace contaminant control
VOC = volatile organic compound
cm = centimeter
°C = degree Celsius
D = depth
°F = degree Fahrenheit
ft = foot
h = hour
H = height
in^3 = cubic inch
kg = kilogram
kPa = kilopascal
lb_m = pounds mass
Lpm = Liter per minute
m = meter
mg = milligram
mm = millimeter
Pa = pascal
ppm = parts per million
psia = pounds force per square foot absolute
scfm = standard cubic foot per minute
W = Watts, width
µm = micrometer
% = percent, percent by volume

I. Introduction

THE National Aeronautics and Space Administration's (NASA) Advanced Exploration Systems (AES) Program has been studying and developing candidate atmosphere revitalization (AR) subsystem equipment architectures that enable future crewed deep space exploration missions.[1-3] Evolving the International Space Station (ISS) AR subsystem architecture has been proposed as a leading strategy to economically advance environmental control and life support (ECLS) technology to meet exploration performance goals.[4] Therefore, the ISS AR subsystem has served as the starting basis for developing the AR subsystem of the future.

A significant component of the technology development efforts has been a series of integrated tests conducted by the AES Atmosphere Resource Recovery and Environmental Monitoring (ARREM) Project. The testing series began with the Resource Recovery Functional Demonstration (R2FD) test to establish the basis for comparison. The R2FD test used ISS AR subsystem flight-like developmental hardware configured according to the ISS AR subsystem architecture. The ARREM Project's Cycle 1 and Cycle 2 tests used many of the same test articles as the R2FD test but configured differently to evaluate targeted functional improvements and subsystem complexity reductions. The R2FD and Cycle 1 tests are discussed in Ref. 5. The following discussion describes the Cycle 2 integrated testing architecture and summarizes the testing results relative to the Cycle 1 testing series.

II. Test Configuration Overview

The ARREM Project Cycle 2 integrated test configuration, depicted by Fig. 1, included the following process equipment:

1) A Trace Contaminant Control (TCC) adsorbent cartridge fixed bed (ACFB) assembly (Calgon Carbons, Barnabey Sutcliffe Division) packed with a candidate adsorbent media (Ammonasorb II, Calgon Carbons).
2) A TCC Microlith®-based high temperature catalytic oxidizer assembly (M-COA) (Precision Combustion, Inc.)
3) A Carbon Dioxide Removal Assembly Version 4 engineering unit (CDRA-4EU) (Honeywell) with beds packed according to the ISS CDRA-4 configuration. This included using adsorbent media obtained from the batches used for the CDRA-4 flight hardware.
4) A Sabatier Development Unit (SDU) carbon dioxide (CO_2) reduction assembly (United Technologies Aerospace Systems).
5) A CO_2 Management Assembly (CMA) consisting of a compressor (Southwest Research Institute) and accumulator tanks were located downstream of the CDRA-4EU equipment to condition the product CO_2 and to serve as a collection buffer that dampens flow rate pulses to the SDU.
6) A developmental Oxygen Generation Assembly (dev-OGA) (United Technologies Aerospace Systems).

This testing configuration was supported by facility support equipment that provided temperature and humidity control, space vacuum simulation, avionics cooling, and metabolic load simulation functions.

A. Differences between Cycle 1 and Cycle 2 Test Architectures

The primary differences between the Cycle 1 and Cycle 2 AR subsystem architectures are found in the TCC and CO_2 removal equipment. Specifics associated with these changes are shown schematically by Fig. 2 and described by the following summary.

The TCC architecture evaluated during Cycle 1 included a Low-flow Fixed Bed (LfFB) assembly containing Chemsorb 1425 (Molecular Products) positioned in parallel with the condensing heat exchanger. The inlet flow for the LfFB originated downstream of the cabin fan and upstream of the condensing heat exchanger. Its exhaust joined the cabin ventilation duct downstream of the condensing heat exchanger. Flow through the LfFB was 8.5 m^3/h (5 ft^3/minute). A small booster fan was required to achieve the desired flow.

Using the booster fan was not desirable so alternatives were sought to provide the trace contaminant control function while utilizing only the cabin ventilation fan. To achieve this objective, the Cycle 2 subsystem architecture consisted of an ACFB assembly which consisted of three activated carbon cartridges containing Ammonasorb II (Calgon Carbons) arranged in parallel just upstream of the cabin ventilation fan. The full cabin ventilation flow of approximately 850 m^3/h (500 ft^3/minute) flowed through the ACFB assembly. The advantage of the ACFB concept over the LfFB was the potential to remove trace contaminants from the full ventilation flow upstream of CO_2 removal, M-COA, and condensing heat exchanger equipment which may experience fouling challenges. The potential to also remove contaminants that may excessively load humidity condensate leading to higher costs to operate water processing systems was also an attractive feature.

The M-COA inlet flow originated from the CO_2 removal unit just downstream of the blower. Its exhaust was directed to the CO_2 removal unit's inlet in the Cycle 1 architecture. For the Cycle 2 architecture, the M-COA inlet flow arose from the cabin ventilation duct downstream of the ACFB assembly and cabin fan. The M-COA exhaust was directed to the CO_2 removal equipment inlet. The advantage of this configuration is that the catalytic oxidation stage is more exposed to the cabin trace contaminant load and therefore can provide greater overall function to remove low molecular weight volatile organic compounds (VOC) that are challenging for the adsorbent bed component of the trace contaminant removal architecture. In contrast, in the Cycle 1 architecture the M-COA was isolated from the low molecular weight VOCs because the process air flow passed through the CO_2 removal unit's desiccant bed upstream of the M-COA inlet interface. The CO_2 removal unit's desiccant material effectively removes many low molecular weight VOCs and oxidation catalyst poisons. While the M-COA is protected from catalysts poisons, it cannot assist with controlling the low molecular weight VOC load. Although methane, carbon monoxide and hydrogen which are the primary compounds targeted for control by the M-COA pass through the desiccant bed, isolating the M-COA from the low molecular weight VOC trace contaminant load components is undesirable from an operational capability perspective. The Cycle 2 architecture sought to correct this situation.

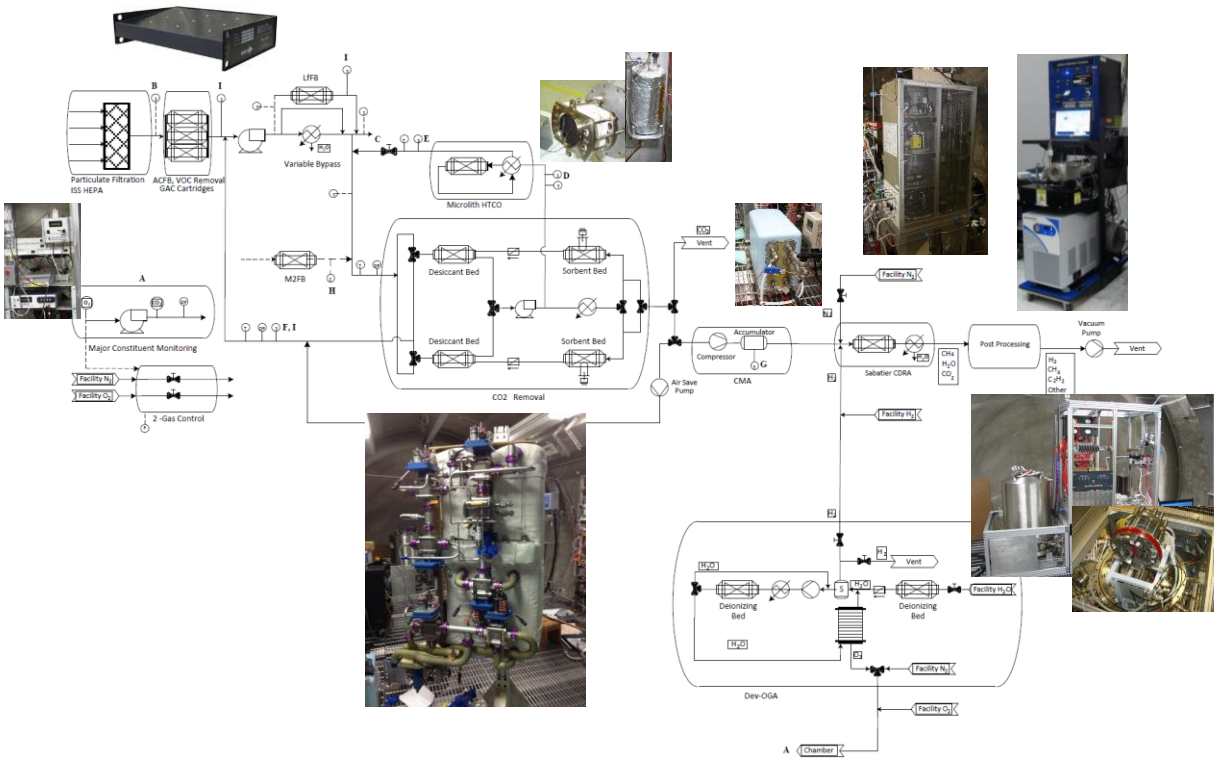

Figure 1. ARREM Project Cycle 2 integrated testing architecture. *Trace contaminant control system components include high flow, low aspect ratio cartridges mounted in the ventilation duct. The CO_2 removal test article was upgraded to CDRA-4 fidelity. Plasma pyrolysis carbon dioxide reduction post-processing was added.*

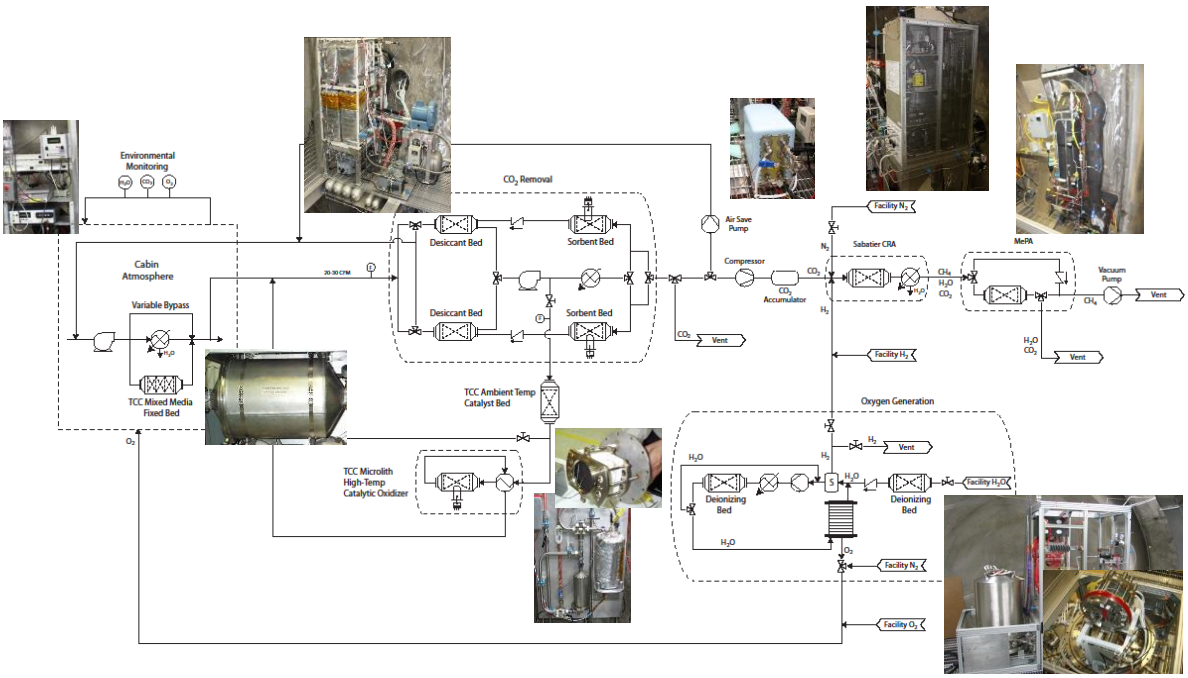

Figure 2. ARREM Project Cycle 1 integrated testing architecture. *Differences with the Cycle 2 testing architecture include 1) different trace contaminant control component types, 2) different trace contaminant control component positioning in the architecture, and 3) lower fidelity CO_2 removal process equipment.*

The CO_2 removal equipment was modified significantly for Cycle 2. During Cycle 1, a developmental CO_2 removal unit that contained flight-like adsorbent media was used. This developmental unit had significant differences from the ISS CDRA relative to desiccant and adsorbent bed aspect ratios and the process air duct configuration. An engineering unit for the ISS CDRA was built that corrected these differences. All process air ducts, desiccant bed, and adsorbent bed components were fabricated and configured according to flight hardware drawings. The engineering unit did incorporate commercially-available ball valves in place of the selector valves and used an externally-mounted commercial blower to allow for greater flow capability than a flight-like vane axial mixed-flow blower. The air saving pump used in the engineering unit was a flight-like research grade unit.

B. Cycle 2 Test Series Phases

The Cycle 2 testing series was conducted in six phases that varied in complexity. The testing phases and their primary objectives were the following:

1) Phase 1—Demonstrate selected dev-OGA control modifications and integrated "recombiner" performance.
2) Phase 2—Demonstrate major constituent monitoring and 2-gas chamber pressure control performance.
3) Phase 3—Demonstrate CDRA-4EU four point test series with and without M-COA integration, demonstrate low CO_2 partial pressure control capability, and demonstrate 9 crewmember support capability.
4) Phase 4—Evaluate trace contaminant control concept architectures.
5) Phase 5—Demonstrate full subsystem architecture with step-wise metabolic challenges at 3-, 4-, and 6-crewmember loads.
6) Phase 6—Demonstrate full subsystem architecture with 4-crewmember dynamic metabolic load.

III. Testing Facility and Methods

The testing facility used for the Cycle 2 testing series is located in a 9,290-m^2 (100,000 ft^2) high-bay area containing bench-scale and sealed chamber testing platforms that allow a full range of testing capabilities ranging from bench-scale demonstration of individual components and assemblies through fully-integrated subsystems and systems. Since 1985, the facility has been instrumental in the development, performance evaluation, and sustaining engineering support for the ISS ECLS system equipment as well as evaluating new technical developments in ECLS system process technologies and integrated architectures.

A. Test Chamber Overview

The 90.6-m^3 (3,200 ft^3) Environmental Control Chamber (EChamber), shown by Fig. 3, provided the integrated testing infrastructure during the Cycle 2 integrated testing series as well as the earlier R2FD and Cycle 1 testing series. The EChamber is outfitted with test support equipment to inject trace chemical contaminants; to provide chamber ventilation, temperature, and humidity control; to provide chamber atmospheric pressure control; to simulate human metabolic loads and demands; to monitor the chamber's internal conditions; to provide a space vacuum simulation resource; and to accommodate thermal and power loads in support of assembly-level and system-level integrated tests. Automated test operations control and data acquisition are provided via LabVIEW (National Instruments) software and data archiving is provided by the Payloads and Components Real-time Automated Test System (PACRATS) software (NASA). The EChamber atmospheric pressure is selectable from slightly above local barometric pressure to <55.2 kPa (<8 psia). An enclosure surrounds the EChamber to minimize the effects of external temperature changes in the facility high bay on the EChamber's internal pressure. During testing the targeted pressure range was 400-933 Pa gauge (0.060 – 0.14 psig) while the targeted temperature was 21 ± 2.8 °C (70 ± 5 °F). The relative humidity target was 50 ± 5%.

Figure 3. EChamber showing Cycle 2 integrated AR subsystem equipment. *The architecture was demonstrated in multiple phases.*

B. Analytical Method Overview

The EChamber's in-line analytical methods provide data necessary for determining that the test objectives are being met. The analytical instrumentation used during the R2FD and ARREM Cycle 1 and Cycle 2 testing series can be divided into two groups—instruments used for trace contaminant propagation studies and instruments used to monitor major constituents of the chamber atmosphere. The trace contaminant monitoring instruments were located in the large high bay facility outside the EChamber enclosure. The temperature inside the high bay was maintained at approximately 23 °C (73 °F) throughout the duration of the tests. Sample delivery from the EChamber to the trace contaminant instrumentation was accomplished via a 6.4-mm (0.25-inch) diameter × 12.2-m (40-ft) long stainless steel, unheated transfer tubing. This tubing was solvent-cleaned and extensively purged with dry nitrogen (N_2) prior to being placed into service. The sample flow was provided by a small pump located near the analytical instrumentation. A multiport valve provided flexibility with respect to sampling location inside the EChamber. The major constituent analysis instruments were mounted inside the EChamber. These instruments sampled the EChamber atmosphere directly, requiring no transfer lines.

1. Trace Contaminant Monitoring Methods

All quantitative analyses with respect to trace contaminants were carried out with an Agilent 6890 gas chromatograph (GC) utilizing a single analytical column and a flame ionization detector. The column was a 30-m (98.4 ft) long intermediate polarity capillary column with a 0.53-mm inner diameter. The film thickness was 3.0 µm. Ultra high purity helium (He) was used as the carrier gas. Facility grade N_2 was used to perform instrument blanks between sample runs.

Sample concentration and delivery to the GC was accomplished with a Markes TT24-7 Thermal Desorption System. This is an electrically cooled, two-trap system with the traps operating sequentially. The measurements were accomplished by sampling from each sample port for 10 minutes during an approximate 25-minute cycle. The traps were packed with Tenax TA™ and Unicarb™ in order to retain both low and high volatility compounds.

The airborne concentration inside the EChamber for the VOCs generated from the liquid injection mixture were expected to be in the low parts per million (ppm) range. The exception being during the initial EChamber conditioning at the start of the test once the door had been closed and sealed. This step was necessary in order to passivate the inner surfaces of the EChamber itself as well as the various items of hardware contained inside. The initial spiking was achieved by using multiple 1-ml injections in rapid succession.

All analytical target compounds were calibrated using standard multipoint methods. During the ARREM Cycle 2 test series, GC calibration was achieved using gas phase standards generated on demand via a National Institute for Standards and Technology (NIST)-traceable permeation tube gas generator manufactured by Kin-Tek. While the GC method error was compound specific, overall, the order of magnitude was in the 25% – 30% range.

A second GC, an Agilent 7890 utilizing a single analytical column with both a flame ionization and a mass selective detector (MSD), was employed for screening and unknown compound identification during portions of the ARREM Cycle 2 test series. This GC was coupled with a Gerstel Thermal Desorption System and in the future will be used in conjunction with the Agilent 6890/Markes 24-7 system to provide more robust testing capabilities than were previously possible.

A Fourier transform infrared (FTIR) spectrometer (Gasmet DX4040) was used for analyzing target compounds near real-time. The Gasmet DX4040, which was identified by commercial market analysis for portable VOC analyzers, is capable of simultaneously monitoring up to twenty-five infrared-active compounds. Specific VOC compounds monitored included acetaldehyde, acetone, dichloromethane, ethanol, isopropanol, methanol, and xylene. Water vapor percent and well as CO_2 and CO were also monitored. Sampling was accomplished via 9.1 m (30 ft) of 6.35 mm (0.25-inch) stainless followed by 3.05 m (10 ft) of 6.35 mm (0.25-inch) Teflon tubing. A sample pump internal to the Gasmet DX4040 FTIR supplied a flow rate in excess of 1 Liter/minute (Lpm). A typical sample cycle consisted of pumping atmospheric air from the EChamber to the FTIR and through the FTIR sample cell for 5 minutes and after disengaging the sample pump, performing spectrum acquisition for 5 minutes. The pump would then re-engage and the cycle would repeat. Sample effluent was returned to the EChamber via a line so that a closed loop could be maintained. Other than for daily re-baselining the instrument with nitrogen (N_2), sampling was usually performed non-stop. The Gasmet DX4040 provided a more rapid sampling rate than the GC units. Analytical results indicate that when compared to the GC-MS, the Gasmet DX4040 tended to overstate the actual concentration present by an average of 10% to 40%, especially for water-soluble compounds such as alcohols. In the case of CO_2 and CO, the unit produced results within the range of other CO_2 and CO monitors used in the testing facility.

2. Major Constituent Analysis Instrumentation

The major constituents monitored during the ARREM Cycle 2 test series included oxygen (O_2), CO_2, and humidity. An instrument array demonstrated in 2002 through 2003 and described by Ref. 6 provided the function. In this array, O_2 was monitored using an Oxigraf Model O2 analyzer. This device utilizes a solid-state laser diode absorp-

tion system and measures O_2 concentrations ranging from 0.01% to 100% by volume. Carbon dioxide was monitored using a Sable Systems CA-2A analyzer, which utilizes solid-state infrared absorption technology and can measure between 1 ppm and 10% CO_2. Relative humidity was measured using a Sable Systems RH-100 meter, employing a solid-state, thin film capacitance detection system. This instrument is capable of measuring relative humidity between 0.01% and 99%. The instrument array performance was stable throughout the ARREM Project Cycle 2 testing series.

Table 1. Contaminant Injection Rates.

COMPOUND	INJECTION RATE (mg/h)	
	Targeted	Actual
Methanol	26.2	44.9
Ethanol	159.9	274.0
2-propanol	11.2	19.2
Ethanal	17.4	29.8
1,2-/1,3-dimethylbenzene	5.4	9.2
Dichloromethane	3.1	5.3
2-propanone	14.4	24.7
Methane	65.2	38.6
Carbon monoxide	9.0	13
Trimethylsilanol	3.9	9.2
Hexamethylcyclotrisiloxane	40.6	69.6

C. Contaminant Injection

A trace Contaminant Injection System (CIS) was provided as facility support equipment to continuously inject gaseous and liquid contaminants into the chamber atmosphere. The CIS continuously injected volatile chemicals which are liquids at ambient temperature and pressure into a closed flow loop where they flash evaporated. The liquid chemicals could be injected individually or in a mixture. Gaseous contaminants were injected using peristaltic pumps attached to bags containing the pure compound gas. Methane, hydrogen, and carbon monoxide were injected by this method. Table 1 lists chemicals injected into the EChamber during Cycle 2 testing Phases 4 through 6.

Table 2. Metabolic production rates.[7]

COMPOUND	ACTIVITY	RATE (kg/CM-h)
H_2O	Sleep	0.0378
	Normal	0.0706
	Exercise	0.629
	Post Exercise	0.281
CO_2	Sleep	0.027
	Normal/Post Ex.	0.047
	Exercise	0.3
O_2	Sleep	0.022
	Normal/Post Ex.	0.038
	Exercise	0.24

D. Metabolic Simulation

A facility-provided metabolic simulator was used to inject water (H_2O) and CO_2 and remove O_2 consistent with multiples of single person daily average rates as static or dynamic challenges. Simple 24-hour average metabolic loads for 1-CM derived from Table 2 are 0.083 kg/h (0.18 lb_m/h) H_2O, 0.047 kg/h (0.104 lb_m/h) CO_2, 0.038 kg/h (0.084 lb_m/h) O_2.[7]

E. Test Data General Error Analysis Overview

The importance of having an accurate mass balance determination for O_2 and the other major constituents—CO_2 and H_2O—cannot be over emphasized. The ARREM Project's goal of developing a regenerable closed-loop ECLS system required that there be minimal error in the test instrumentation. One of the most important aspects of a regenerable system is recovering sufficient O_2 and H_2O to survive in space when resupply from Earth is no longer possible or feasible. Having sufficient supplies, or tolerances for the major constituents, is imperative and understanding the mass balance general uncertainty is important to defining tolerance magnitude for exploration missions.

At the conclusion of the Cycle 1 testing series, a generalized uncertainty analysis was conducted by the ARREM Project to understand test instrumentation error propagation and prepare for the Cycle 2 testing series. The ARREM Project based its error analysis for the integrated system on Ref. 8 which discusses the propagation of errors within an experiment and covers bias, precision error, varying sample size, varying orders (zeroth-nth), and transient versus steady-state experiments.

Manufacturer data sheets disclosing sources of error for the instrumentation utilized in the ARREM Project's Cycle 1 integrated testing configuration were acquired to determine the primary measurement errors. The instrumentation manufacturers also provided instructions on how to calculate respective instrumentation error on each data sheet. Instrumentation error is a percentage of the instrument readings added to a percentage of the full scale (FS) of the instrument. The ARREM Project recorded its instrument readings using the PACRATS data acquisition soft-

ware. The applicable test data were then selected, downloaded, and analyzed. Each parameter was assigned an instrument and had a unique identifier.

Results from the generalized error analysis applied to the Cycle 1 integrated test mass balance found that the mass flow control and measurement sensors used for simulating the metabolic CO_2 load and O_2 demand contribute the greatest to the overall error in the mass balance. Propagated error associated with the CO_2 mass balance found that the error associated with the simulated metabolic CO_2 load ranged between 0.054 kg (0.12 lb_m) and ±0.894 kg (±1.97 lb_m). The discrete mass balance differential on CO_2 was within 0.50 kg (1.1 lb_m) on average during integrated testing phases. The higher error was associated with an error component applied to the discrete measurement itself. Because the flow instrumentation consisted of a mass flow totalizer, a mass totalizer value starting at a high discrete value resulted in a larger error component than when the totalizer was re-set to a lower starting discrete value. Propagated error associated with the simulated O_2 production ranged between ±0.68 kg (±1.5 lb_m) and ±1.95 kg (±4.3 lb_m) which represented over 90% of the total O_2 mass balance error. The discrete O_2 mass balance differential was within 0.44 kg (0.96 lb_m) on average during testing. Similarly, for the water mass balance the production load error ranged between ±0.11 kg (±0.25 lb_m) and ±0.33 kg (±0.72 lb_m) which accounted for over 90% of the total H_2O mass balance error. The discrete mass balance on water was within 0.68 kg (1.5 lb_m) during integrated testing phases. These findings indicated that the instrumentation associated with metabolic simulation accounted for the greatest portion of the total mass balance error. Therefore, more precise instrumentation for simulating metabolic loads and demands can benefit the testing results. Metabolic simulation instrumentation improvements were not made in preparation for the Cycle 2 testing series; therefore, the propagated instrumentation error associated with overall mass balance during the Cycle 1 testing series applied to the Cycle 2 testing series.

IV. ARREM Cycle 2 Testing Series Results

Results from each testing phase are summarized in the following discussion. Focal areas include oxygen generation, carbon dioxide removal, trace contaminant control, and integrated AR subsystem performance.

A. Phase 1 Oxygen Generation Assembly Alternative Configuration Demonstration

Phase 1 focused on specific O_2 generation equipment operational and physical configuration changes to partially or fully address technical aspects pertaining to the following:

1) Demonstrate an operational approach with an alternative (or no) hydrogen sensor
2) Demonstrate an operational approach leading to eliminating the cell stack containment dome
3) Demonstrate an approach to eliminate the nitrogen purge
4) Demonstrate a recirculation loop flush/sampling capability
5) Demonstrate the effects of different current levels
6) Demonstrate a cell discharge procedure
7) Demonstrate an approach to eliminate the wastewater interface

Detailed results obtained from this testing phase are provided by Ref. 9.

Phase 1 investigated whether the OGA can be safely operated without startup or shutdown N_2 purges by making use of H_2 and O_2 recombination that occurs naturally at the anode catalyst sites. The test consisted of three 1-week runs that included a baseline run with both purges, a run with the startup purge disabled, and a run with both the startup and shutdown purges disabled. Each of the N_2 purge deletion tests were conducted twice for repeatability which was observed. The overall conclusion is that disabling N_2 purging does not appear to introduce new safety risks to operating the OGA. Eliminating the N_2 purging for an exploration OGA eliminates ~22.7 kg (~50 lb_m) equipment mass and volume associated with the purge. Additional exploration mission mass reduction associated with spare parts may also be realized. According to analysis conducted by the White Sands Test Facility the resulting explosion magnitude would release energy equivalent to a single firecracker if no H_2/O_2 recombination occurs.[10] It was noted that water in the oxygen outlet that results from the H_2/O_2 recombination process needs to be removed to prevent damage to downstream H_2 sensors or recombiners.

B. Phase 2 Major Constituent Monitoring and Chamber Pressure Control Demonstration

The EChamber was outfitted to include a total pressure and O_2/N_2 partial pressure control capability. The equipment configuration to provide the major constituent composition control and chamber total pressure control were exercised through several cycles. The equipment employed a flight-like control algorithm used aboard the ISS. Phase 2 successfully demonstrated a facility-provided test support function which enabled later testing phases. Because Phase 2 was test support centric instead of AR Subsystem technology centric, the details are not discussed here.

C. Phase 3 Carbon Dioxide Removal Assembly Engineering Unit Performance Mapping

The CDRA-4EU evaluated during Phase 3 possessed high functional and configuration fidelity compared to the ISS CDRA-4. The CDRA-4EU CO_2 sorbent bed was filled with RK38 zeolite 5A (Honeywell UOP) obtained from the flight material lot while the desiccant bed was a layered arrangement consisting of zeolite 13X (Honeywell-UOP) occupying 44.4% of the bed volume and Sylobead SG 125 B silica gel (W.R. Grace & Co.) occupying 46.5% of the bed volume. After completing testing to establish baseline performance relative to previous tests shown by Fig. 4, the potential for increasing the CO_2 removal performance by increasing the process flow rate was investigated. The nominal flow of 34.7 standard m^3/h (20.4 standard ft^3/minute or scfm) was increased to approximately 42.5 standard m^3/h (25 scfm) while the cycle time was reduced from 144 minutes to 90 minutes which is the minimum time required for the CO_2 sorbent beds to heat to the nominal set point of 204.4 °C (400 °F). Performance results from this test, shown in Fig. 5, were favorable for maintaining cabin CO_2 levels to <2 mm Hg (2,667 ppm or 0.27%) under a 4-crewmember load. Removal capacity for a 9-crewmember load was also demonstrated. This was the 5 mm Hg (6,579 ppm or 0.66%) challenge case. Carbon dioxide sorbent bed breakthrough was experienced at this loading condition as shown by the decrease in removal efficiency from the 4 mm Hg (5,263 ppm or 0.53%) case. The combination of higher flow rate and reduced cycle time, however, resulted in considerably higher power requirements. Average heater power alone increased by 200 Watts compared to a nominal flow rate and half cycle settings. Blower power was not measured yet it is expected to also increase significantly.

As part of Phase 3, the flow balance between the M-COA and CDRA-4EU equipment was established.

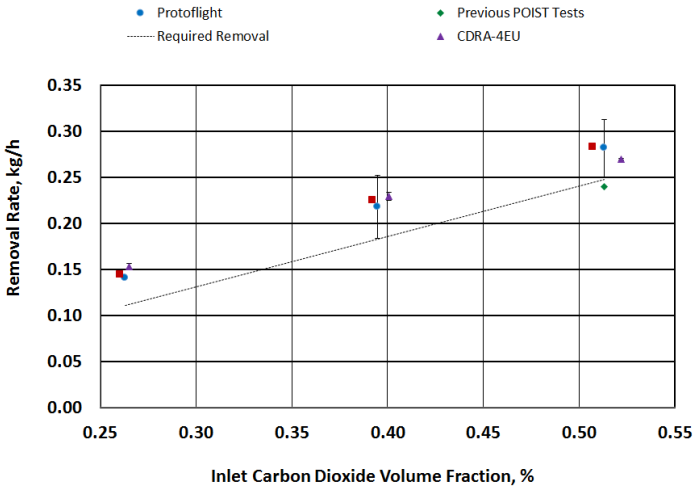

Figure 4. Carbon dioxide removal engineering unit equipment performance. *Very good agreement with protoflight and developmental unit performance was observed.*

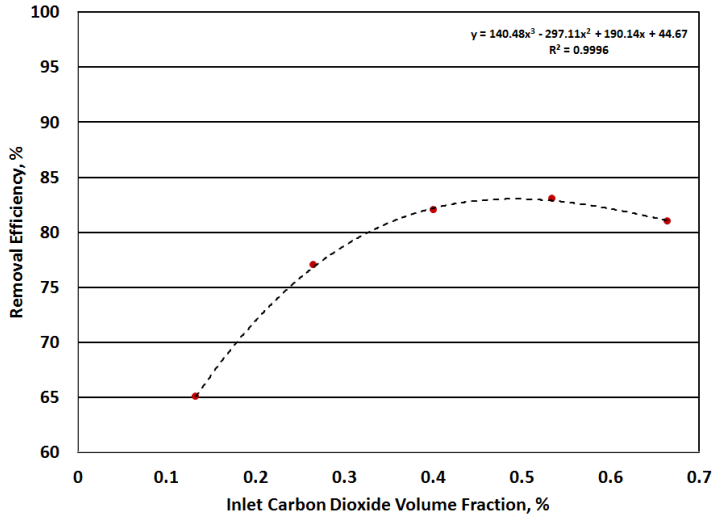

Figure 5. Carbon dioxide removal engineering unit equipment performance at 42.5 m^3/h. *The CO_2 adsorbent beds did not break through below inlet CO_2 partial pressure <5 torr.*

D. Phase 4 Trace Contaminant Control Alternative Demonstration

Phase 4 demonstrated the function of the ACFB assembly versus the low-flow fixed bed (LfFB) assembly used during Cycle 1. The EChamber ventilation system, condensing heat exchanger, and contaminant injection equipment was included in the testing phase. The testing was conducted under conditions that prevented humidity condensation to ensure that the adsorbent bed removal was the sole control mechanism. Contaminant and humidity injection established an initial condition and the ventilation system was operated to provide chamber atmospheric mixing. The trace contaminant concentrations were monitored during the testing phase to determine the performance of the ACFB and LfFB concept architectures.

During test Phase 4, each architecture was operated independently. Although, each adsorbent bed configuration contained similar quantities of activated carbon (~23.5 kg for the ACFB and 21 kg for the LfFB) each bed varies in process air flowpath and aspect ratio. The ACFB, consisting of three vertically-stacked cassettes 15.24 cm H × 60.96 cm W × 35.56 cm D (6 inches H × 24 inches W × 14 inches D) with a volume of 13.52 liters (825 in^3) of Ammonasorb II (4 × 8 mesh) each, resided on the inlet of the main ventilation ductwork and saw the full 849.5 standard m^3/h (500 scfm) ventilation flow while the LfFB, a 33.02-cm diameter × 38.10-cm long (13-inch diameter × 15-inch long) cylindrical bed with a volume of 32.63 liters (1991 in^3) packed with Ammonasorb II (6 × 12 mesh), received only 20.39 standard m^3/h (12 scfm) of the ventilation flow via a side branch.

Both computer simulation and intuitive experience suggested low molecular weight compounds such as methanol and acetaldehyde would break through both the ACFB and LfFB. This was observed during in both cases. Computer simulations also suggested the ACFB would maintain good single pass efficiency for siloxane compounds. Experimental data showed that as late as test day 6 into Phase 4 testing that the ACFB still maintained a capacity for siloxane and organosilicone compounds which maintained the chamber atmospheric concentration near or below facility analytical instrument detection limits. Performance was also maintained for xylene. In addition, acetone and isopropanol were held at lower concentrations compared to the LfFB. This was in part due to the much higher flowrate through the ACFB increasing chamber scrubbing rates. It was thought that this high flow would also promote early breakthrough; however, the observed breakthrough was much lesser extent than predictions indicated.

Due to the low trace contaminant concentrations maintained during the ACFB phase and considering in particular its ability to still control the lowest molecular weight cyclic siloxane, hexamethylcyclotrisiloxane (D3 siloxane), the ACFB was selected for further testing in Phases 5 and 6 to characterize its breakthrough profile. Although the LfFB also maintained high efficiency for siloxane removal, the novelty and potential applicability of the ACFB concept to mitigate trace contaminant problems aboard ISS attributed to siloxanes and other high molecular weight compounds made the ACFB an attractive option to further test. As the test progressed and more compounds broke through the ACFB, the chamber concentration profile changed. Breakthrough at the high ACFB velocity appeared to be molecular weight dependent with the heavy D3 siloxane and xylene remaining under control. Conversely, the LfFB maintained high single pass efficiency throughout the test but due to its low flowrate only a small amount of the cabin atmosphere could be effectively scrubbed of chemical at any given time. Testing results indicate that exploration AR subsystem architectural considerations may benefit from using both an ACFB and an LfFB combined with a catalytic oxidation stage.

E. Phase 5 Core Architecture Performance Mapping

The core AR equipment consisting of the CDRA-4EU, TCC equipment, CMA, SDU, and dev-OGA was challenged with static metabolic challenges progressing through levels equivalent to 3, 4 and 6 crewmembers. Each metabolic challenge was maintained for 48 hours minimum. Trace contaminant injection and monitoring was conducted during the testing phase to understand the fate of specific chemical contaminants in the core architecture. The leakage from the EChamber averaged 1.08 kg/day (2.38 lb_m/day) during the testing phase. The EChamber O_2 level was maintained much better in Cycle 2 than during the Cycle 1 testing series with only a 0.6% variance during Phase 5. The EChamber dew point was maintained between 15 °C and 20 °C (60-65 °F) which is comparable to Cycle 1 conditions.

1. *Trace Contaminant Control*

The ACFB, M-COA, and the condensing heat exchanger were the primary contaminant removal equipment operating during Phase 5. Figure 6 shows that the ethanol concentration slowly rose from an initial concentration of 2 ppm to just over 4 ppm by the end of test day six which was still well below the 180-day Spacecraft Maximum Allowable Concentration (SMAC) of 1,000 ppm. The same can be said for CH_4 which peaked at 55 ppm compared to its 180-day SMAC of 5,300 ppm. Carbon monoxide (CO) exhibited the same slow rise topping out at 17 ppm which is still below the 55-ppm 7-day SMAC but above the 15-ppm 30-day/180-day/1,000-day SMAC. The latter SMAC of 15 ppm is the target for exploration missions.

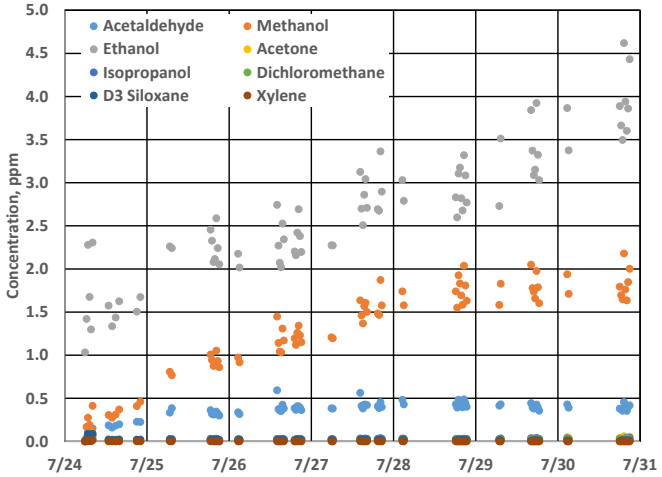

Figure 6. Phase 5 EChamber atmospheric load.

The concentration trends for ethanol and metha-

nol were indicative of ACFB breakthrough. This breakthrough was expected for the low molecular weight compounds. ACFB performance indicated high single pass removal efficiencies for xylene and D3 siloxane. Xylene removal efficiency was 100% while D3 siloxane removal efficiency was approximately 77%. Isopropanol was removed at around 30%.

Trace contaminant concentration swings were observed during Phase 5 testing. Figure 7 illustrates the VOC load swings in the EChamber during Phase 5 using ethanol as the example. In Fig. 7, the GC-MS data and the FTIR data are overlaid. The FTIR trend line includes all data gathered by the instrument during Phase 5 testing. The selected FTIR data points (Selected Data) are those with a timestamp closely matching that of the GC-MS data. It can therefore be inferred that the scatter is not an instrumental error but a characteristic of the test itself. The apparent concentration offset between the two instruments is a result of both the inherent nature of the FTIR technique as well as a characteristic of the test configuration.

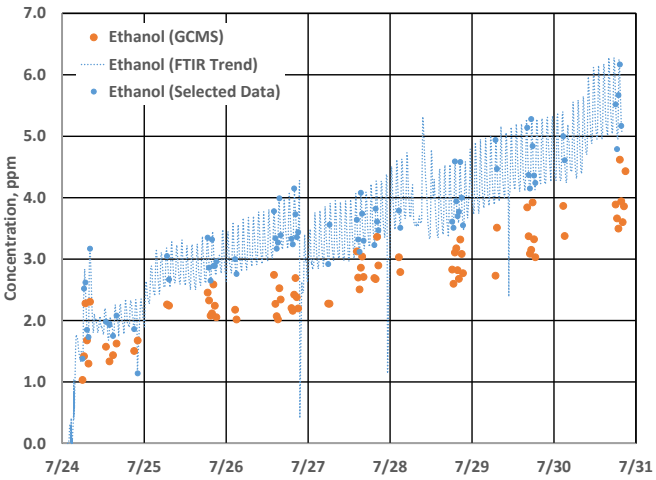

Figure 7. Phase 5 EChamber atmospheric ethanol load as measured by GCMS (~25 minute resolution) and FTIR (10 minute resolution).

The exhaust from the CDRA-4EU returns humidity to the EChamber atmosphere during each desiccant bed regeneration cycle. Analysis downstream of the CDRA-4EU observed highly variable VOC concentrations. Ethanol, methanol, and acetaldehyde were the primary compounds observed. Ethanol concentrations typically ranged between 1 ppm and 12 ppm while methanol concentrations typically ranged between 1 ppm and 5 ppm. A methanol concentration as high as 8 ppm was observed. Acetaldehyde concentrations typically ranged between 0.5 ppm and 1.5 ppm although a concentration as high as 6 ppm was observed. The VOC concentration variability at the CDRA-4EU outlet is believed to result from capturing VOCs on the desiccant beds during their adsorbing phase and subsequently desorbing them along with moisture during the desorption phase. This VOC loaded exhaust from the CDRA-4EU correlated with the periodic ethanol trends observed by FTIR monitoring shown in Fig. 7 and therefore was believed to cause the increase in GCMS data scatter observed in Phase 5 testing.

The CO_2 captured by the CDRA-4EU was supplied to the CO_2 management assembly for compression and storage until needed for reduction by the SDU. This compressed CO_2 was stored in an accumulator tank and sampled periodically for VOC content. The VOC loading in the CO_2 was very low, typically <100 ppb, indicating that compounds were not being retained on the molecular sieve adsorbent. This result was consistent with observations during Cycle 1 testing.

The M-COA's performance was compromised somewhat by a lower than expected throughput—0.5 m^3/h (0.85 scfm) versus the desired 3.4 m^3/h (2 scfm)—and possible siloxane contamination of the catalyst. The unit's temperature profile was also unexpectedly dynamic and tended to be lower than expected. Post-test evaluation found that thermal control of the M-COA is more difficult below 1.7 m^3/h (1 scfm) when using deadband control logic for regulating catalytic reactor temperature. As a result, the M-COA unit operated at an average lower temperature leading to reduced oxidation efficiency. The observed efficiency was found to be consistent with past testing of the unit at a similar temperature. Post-test evaluation also found 94% single pass oxidation efficiency for CO. The thermal dynamics observed may be corrected by implementing proportional-integral-derivative (PID) control rather than the typical deadband control logic. Based on the post-test evaluation, the increasing CO concentration was attributed to an injection rate into the EChamber higher than targeted.

At the testing conditions, the M-COA's performance was quite variable. Complete oxidation of isopropanol was observed. Early in the test phase, the oxidation of ethanol was in excess of 90% but declined towards 73.2% ± 2.6, possibly due to increased chamber loading as the test progressed. Similar behavior was observed for methanol settling out at an efficiency of 78.5% ± 1.3. The oxidation efficiency of acetone appeared to be scattered randomly and the mean efficiency of dichloromethane was low at 11.3% ± 7.0. The mean oxidation efficiency of acetaldehyde was negative at -47.5% indicating it was being generated as a partial oxidation product in the M-COA, likely from ethanol at the lower than expected operating temperature.

Two unexpected observations were made with respect to siloxane compound oxidation. First, the oxidation efficiency of ethoxytrimethylsilane and TMS showed an unexpected trend as these compounds were at first oxidized

effectively. As the test progressed both compounds were exhausted from the M-COA at increasing concentrations that exceeded all know sources. Second, a large negative mean oxidation efficiency at -2,856% ± 751.7 was observed for D3 siloxane indicating net generation of D3 siloxane inside the M-COA. In order to investigate these effects the mass spectra data were scrutinized outside the target compound range of Cycle 2 testing. In addition to D3 siloxane, three additional cyclic siloxanes were identified around the M-COA—octamethylcyclotetrasiloxane (D4 siloxane), decamethylcyclopentasiloxane (D5 siloxane), and dodecamethylcyclohexasiloxane (D6 siloxane).

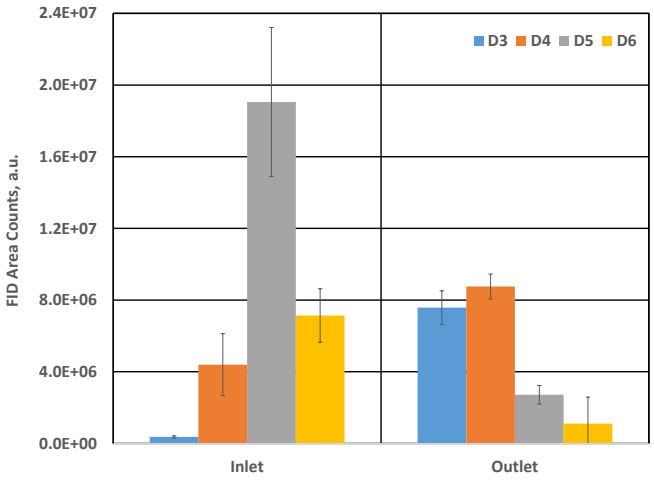

Figure 8. M-COA mean inlet and outlet siloxane loading. *The inlet concentration of D3 siloxane was 0.004 ppm and the outlet was 0.134 ppm.*

Figure 8 displays the mean aggregate M-COA inlet and outlet siloxane abundance during Phase 5 testing. The displayed area counts are uncalibrated flame ionization FID peak areas for compounds other than D3 siloxane. Note that D3 siloxane was the only compound actively injected. It was believed that the source of the D4, D5, and D6 siloxane compounds in the M-COA inlet were offgassing products from newly plumbed hose connecting the M-COA to the main ventilation duct. This was supported by the trend in the inlet D5 siloxane concentration which continuously decreased over the test duration as would be anticipated from an offgassing material. Recall that injected D3 siloxane was removed from the M-COA inlet air stream by the ACFB with 77.1% efficiency. Therefore it does not appear D3 siloxane was being offgassed. As shown by Fig. 9, the two lower molecular weight compounds (D3 and D4 siloxanes) increased in abundance from inlet to outlet whereas the two largest compounds (D5 and D6 siloxanes) decreased. This supports breakdown of D5 and D6 siloxanes by degradation or oxidation to lower membered cyclic siloxane rings. The mass balance of this reaction is unfortunately unknown and there exists the possibility that lighter siloxane fragments such as mono and disiloxane were also generated. The influence of this reaction on the unusual trend in ethoxytrimethylsilane and TMS oxidation efficiency is unknown. In addition fragmentation, to the possibility of complete deposition of SiO_2 on the M-COA catalyst surface also exists. Catalyst masking would be seen by a decrease in M-COA oxidation performance. Indeed, post-Cycle 2 testing of the M-COA revealed only 94% single pass oxidation efficiency for CO. Near 100% CO efficiency was expected at the flowrate and temperatures used in this check. Catalyst masking may explain the decreasing trend in methanol and ethanol oxidation efficiency over time. The reversibility of this effect on the catalyst is unknown.

2. Carbon Dioxide Control and Management

As shown by Fig. 9, the EChamber CO_2 concentration was maintained at lower concentrations compared to Cycle 1. The Cycle 2 conditions achieved ranged between ~0.25% (2,500 ppm) and 0.45% (4,500 ppm) when operating the CDRA-4EU at the selected 42.5 m^3/h (25 scfm) flow and 90-minute half cycle condition. At these conditions the CDRA-4EU maintained the CO_2 partial pressure below the 1,000-day SMAC for all metabolic challenge cases as illustrated by Fig. 9. As noted during the Phase 3 testing, achieving this performance costs approximately 200 W average power due to a higher bed heater duty cycle. The additional power required by the blower to achieve the flow condition was not measured.

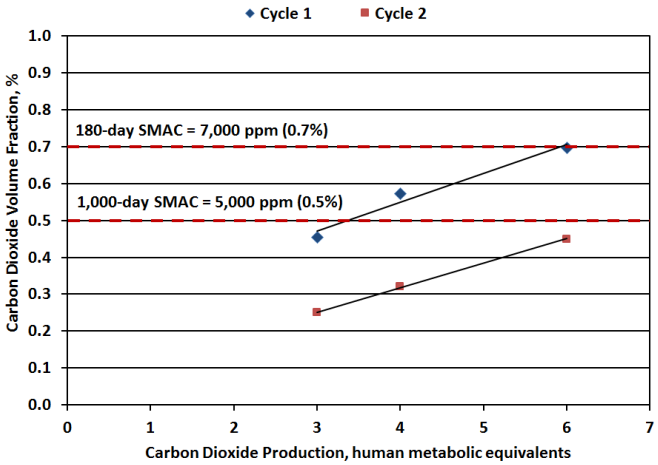

Figure 9. Comparison of Average CO_2 partial pressure plateau concentrations during the ARREM Cycle 1 and Cycle 2 tests. *Single person CO_2 production basis is 0.042*

The CO_2 Management Assembly was operated according to a flight-like control logic for managing the accumulator pressure. This logic provided for a larger working quantity of CO_2

compared to Cycle 1 testing. Also, sampling from the accumulator tank to measure CO_2 purity was coordinated to significantly reduce the impact associated with gas losses for analytical purposes. The result was that the SDU experienced no processing standbys during Phase 5. There were also very few instances of the CDRA-4EU dumping CO_2 to space vacuum due to a full CO_2 accumulator.

F. Phase 6 Dynamic Metabolic Load Control Demonstration

The sixth testing phase continued the integrated AR subsystem operations but subjected the integrated AR subsystem to a dynamic 4-crewmember metabolic load summarized by Table 3 over a 72-hour period. During this phase, the EChamber atmosphere ethanol concentration settled into a range of 4-8 ppm which is well below the 180-day SMAC of 1,000 ppm. Methane concentration rose to ~33 ppm which is well below the 180 SMAC of 5,300 ppm. Carbon Monoxide rose slowly to a peak concentration just under 12 ppm. This level was below the 55-ppm 7-day SMAC as well as below the 15-ppm 30-day/180-day/1,000-day SMAC. The ACFB, M-COA, and the condensing heat exchanger were the primary trace contaminant removal components for Phase 6 as they were in Phase 5. The testing data indicated that the integrated AR subsystem test articles handled the dynamic metabolic load without anomaly or excursion outside habitable limits. Significantly the peak CO_2 partial pressure was maintained below the 1,000 day SMAC for all metabolic loading conditions as shown by Fig. 10. However, concentrations exceeded the targeted 2 mm Hg (0.27%) level during the simulated exercise periods. Carbon dioxide management, trace contaminant control, SDU, remained consistent with the performance observed during Phase 5. A problem with a power supply caused the dev-OGA unit to shut down during Phase 6 and the test was completed by simulating the oxygen generator's function.

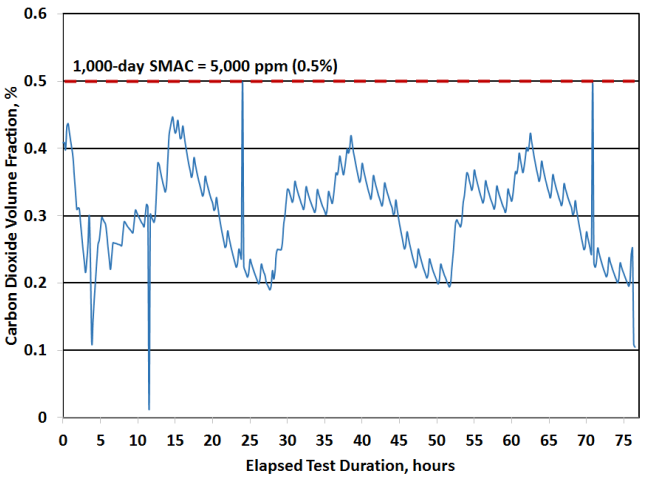

Figure 10. Phase 6 carbon dioxide partial pressure profile. *Concentrations were maintained below the 1,000-day SMAC of 0.5% for all conditions.*

During Phase 6, the trace contaminant control equipment performance remained consistent with the performance observed during Phase 5. Concentrations stabilized at levels shown by Fig. 6 near the end of Phase 5 and continued to exhibit fluctuations that were attributed to CDRA-4EU cycling. A slight upward trend in ethanol and methanol concentration was evident during Phase 6. The ACFB performance was excellent for xylene and D3 siloxane but continued to show signs of breakthrough and roll-up phenomena for other compounds as the testing phase progressed. The D3 siloxane removal efficiency of 75.9% with a standard deviation of 2.3% was remarkably similar to performance observed during Phases 4 and 5. Other organosilicone compounds were removed at slightly reduced efficiencies compared to Phase 5 indicating some breakthrough.

Table 3. Dynamic metabolic load during Phase 6. *The single crewmember basis is provided by the appendix.*

TIME	DURATION (h)	CM1	CM2	CM3	CM4	H_2O (kg/h)	CO_2 (kg/h)	O_2 (kg/h)
0000-0800	8	Sleep	Sleep	Sleep	Sleep	0.151	0.108	0.088
0800-0830	0.5	Exercise	Normal	Normal	Normal	0.841	0.441	0.354
0830-0930	1	Post Ex.	Normal	Normal	Normal	0.493	0.188	0.152
0930-1000	0.5	Normal	Exercise	Normal	Normal	0.841	0.441	0.354
1000-1100	1	Normal	Post Ex.	Normal	Normal	0.493	0.188	0.152
1100-1600	5	Normal	Normal	Normal	Normal	0.282	0.188	0.152
1600-1630	0.5	Normal	Normal	Exercise	Normal	0.841	0.441	0.354
1630-1730	1	Normal	Normal	Post Ex.	Normal	0.493	0.188	0.152
1730-1800	0.5	Normal	Normal	Normal	Exercise	0.841	0.441	0.354
1800-1900	1	Normal	Normal	Normal	Post Ex.	0.493	0.188	0.152
1900-2400	5	Normal	Normal	Normal	Normal	0.282	0.188	0.152

The VOCs where concentrated by the CDRA-4EU in a similar manner as observed during Phase 5. As well, the VOC loading in the CO_2 being delivered to the SDU was at the same magnitude observed during Phase 5.

The M-COA continued to provide complete isopropanol oxidation. However, the mean oxidation efficiencies for methanol (48.5%), ethanol (48.5%), acetone (4.8%) and dichloromethane (2.4%) were lower than during Phase 5. Catalyst masking by SiO_2 is suspected for the decrease since the siloxane behavior observed during Phase 5 continued through Phase 6.

V. Recommended Architecture and Future Improvements

Technical development efforts conducted by the ARREM Project as well as future process development have benefited from multiple contributing technology maturation efforts. The primary process design concepts investigated by the AES ARREM Project originated from an alternative component integration concept proposed in 2004.[11] During the periods before 2004 and between 2004 and 2010, a number of ECLS process technology development and maturation projects made notable progress in the CO_2 removal, trace contaminant control, CO_2 reduction, O_2 generation, and environmental monitoring functional areas. Based on this contributing development work and the work conducted by the ARREM Project, an AR and EM subsystem architecture shown by Figs. 11 and 12 are recommended for further development. The architecture depicted by Fig. 11 is more closely ISS-derived while the architecture depicted by Fig. 12 incorporates alternative CO_2 removal and CO_2 reduction process technologies. The following discussion summarizes features of both architectures.

A. Features of the Recommended AR Subsystem Architecture

Features common to the recommended AR subsystem architectures include core particulate filtration, temperature and humidity control, trace contaminant control, and major constituent monitoring hardware. These AR subsystem architectures must be supported by a robust environmental monitoring subsystem architecture. The core CO_2 removal portion of the architecture is either based on physical adsorption as is used aboard the ISS or thermally regenerable amines. The latter is an extension of the vacuum-swing regenerable amine process included in the Orion vehicle's AR subsystem design.

The particulate removal concept is a 3-stage process consisting of course debris screening, mid-sized particulate filtration, and a high efficiency polishing stage. Debris screening and mid-sized particulate filtration stages are amenable to a distributed architecture and function to keep the main ventilation supply ducts clean. The high efficiency polishing stage concept is envisioned to consist of an indexing media filter assembly closely coupled with the heavy VOC removal stage just upstream of the cabin fan and condensing heat exchanger package.

The trace contaminant control components consist of heavy and light VOC removal stages. The light VOC removal stage also targets methane, hydrogen, and carbon monoxide. These stages are distributed in the architecture. The heavy VOC removal stage concept is a high volumetric flow, low aspect ratio adsorbent cartridge concept derived from a commercially-available design (Calgon Carbons, Barnabey Sutcliffe Division). This cartridge design is packed with a combination of activated carbons formulated to remove ammonia and low concentration VOCs. Leading activated carbon candidates include Ammonasorb II (Calgon Carbons) and OVC carbon (Calgon Carbons). The light VOC removal stage is integrated closely with the core CO_2 removal equipment. This stage consists of a thermal catalytic oxidation reactor coupled with a recuperative heat exchanger. The catalytic oxidation reactor is based on Microlith® technology (Precision Combustion, Inc.). An advanced recuperative heat exchanger design has also been developed and a fully integrated unit designed and fabricated by Precision Combustion, Inc.[12] A small adsorbent bed targeting ammonia, sulfur compounds, and volatile methyl siloxane compounds is positioned upstream of the M-COA.

For the architecture depicted by Fig. 11, the process gas drying and CO_2 removal stages consist of modified versions of the ISS CDRA-4 beds. Alternative adsorbent media and bed sizes tailored to exploration mission metabolic loads are key features. The process must be capable of operating in both open- and closed-loop modes as well as be amenable to deployment across multiple exploration vehicle and habitat platforms. The CO_2 removal stage may contain features of the sorbent-based atmosphere revitalization (SBAR) concept that is capable of simultaneous moisture and CO_2 removal for open-loop applications. Combined with an upstream drying stage that enables water recovery, the system can accommodate closed-loop applications

The architecture depicted by Fig. 12 uses a thermally-regenerated amine process that is being explored to extend vacuum-regenerated amine technology used for open loop architectures such as that for the Orion vehicle to closed loop architectures that are necessary for deep space exploration missions. The process includes a thermally regenerable amine stage to remove CO_2 from the cabin atmosphere. The CO_2 and water that is removed from the process air stream concurrently are sent to a drying stage that operates under a pressure-swing adsorption (PSA) regime. This

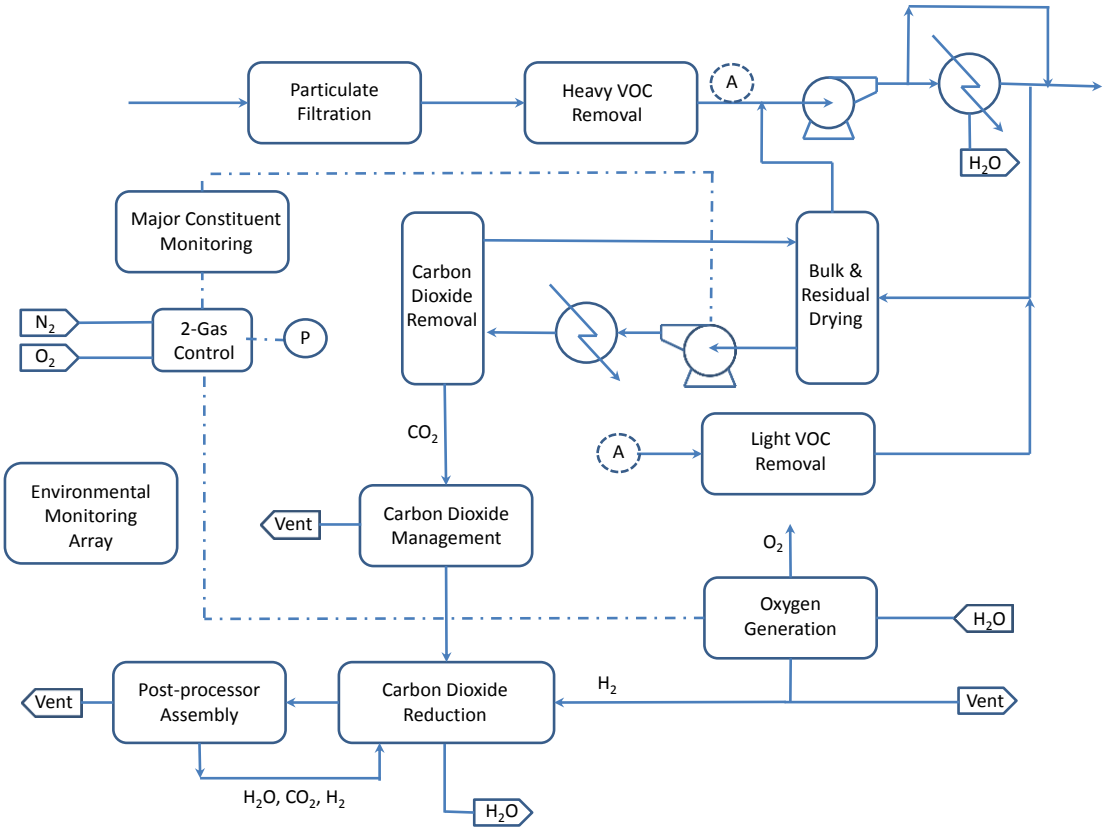

Figure 11. Recommended ARS and EMS architecture.

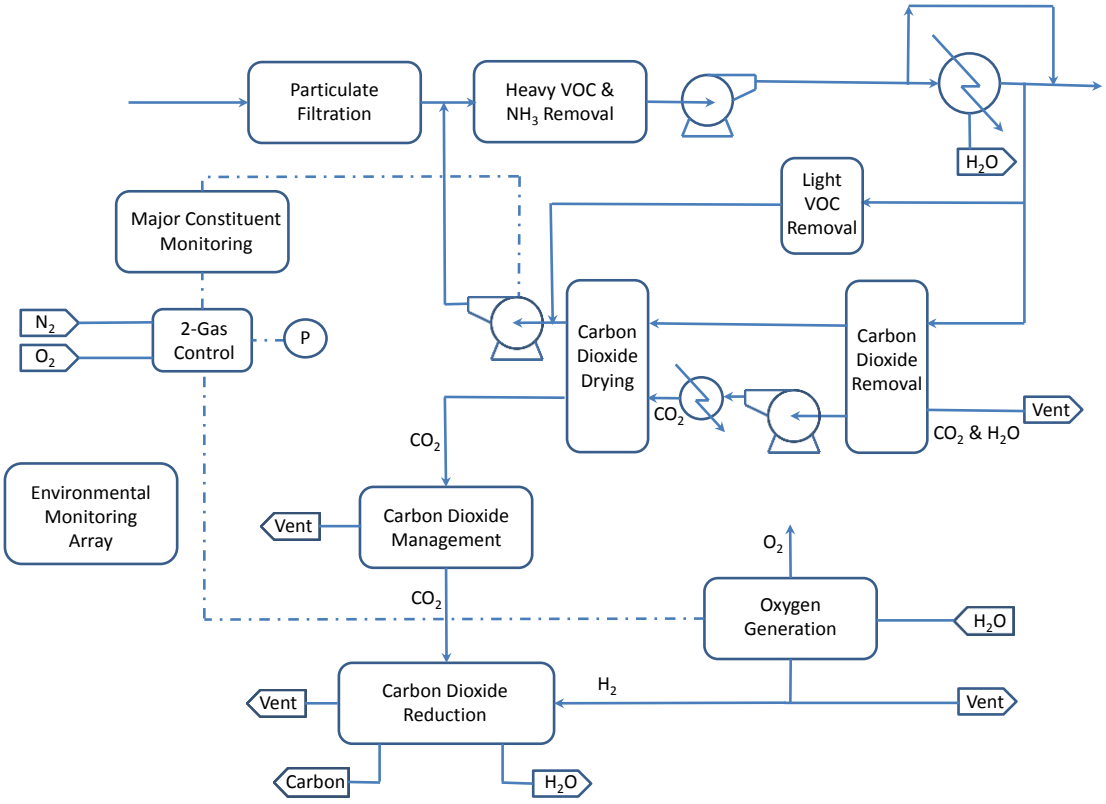

Figure 12. Variant of a Recommended ARS and EMS architecture.

unit could be similar to the isothermal bulk desiccant (IBD) concept considered under a bulk and residual drying concept study.[13] By drying only the CO_2, there is the potential that the drying stage can be smaller than if the full process air stream is dried upstream of the CO_2 removal stage. A first stage blower-compressor provides pressurization of the water-saving PSA and when regenerated the primary CO_2 removal blower provides a regeneration pressure at just below the cabin ambient condition. The CO_2 removal stage is configurable to operate in either open- or closed-loop fashion.

Carbon dioxide management equipment in both architectures consists of a mechanical piston compressor (Southwest Research Institute) and accumulator tanks. This equipment is the ISS state-of-the-art (SOA). An alternative approach uses a temperature-swing adsorption process to combine the CO_2 removal, storage, and compression functions; however, the technical maturity achieved during the ARREM Project has not allowed for a rigorous trade assessment.[14] Further work is necessary to mature the combined CO_2 removal, storage, and compression concept to conduct the necessary functional trade assessment to determine whether replacing the ISS SOA is appropriate.

The oxygen generation functional architecture is predominately the ISS SOA with some operational and equipment updates. Operational changes include operating without a nitrogen purge that reduces equipment complexity and reduces mass. Equipment changes include an electrolytic cell stack that incorporates contemporary chemically-stabilized Nafion™ membrane material and replacing a hydrogen sensor with an advanced sensor technology or using an external catalytic unit that reacts to hydrogen carryover through a temperature increase. The architectures in Figs. 11 and 12 are supplemented by high pressure oxygen generation to support extravehicular activity provided via external compression, either provided by a solid oxide process combined with a mechanical compression stage or a pressure-swing adsorption process combined with a mechanical compression stage. Future development on high pressure water electrolysis is also a candidate for this function. The architectural aspects with these options for supplying high pressure oxygen are likely significant and warrant detailed trade assessment. A secondary consideration is to technology that combines the functions of oxygen generation and CO_2 reduction. Several approaches to achieving this common functionality are funded as Advanced Oxygen Recovery systems. None of these approaches was included in these architectures, but could potentially provide significant decreases in mass, volume, and power requirements for a future architecture approach.

For the architecture depicted by Fig. 11, oxygen recovery is provided via Sabatier-based CO_2 reduction to provide mid-range O_2 resource recovery. A downstream methane plasma pyrolysis process provides further loop closure by converting the methane to a mixture of hydrogen and acetylene.[15] This combination is limited in its degree of loop closure and alternative Bosch-based processes and other carbon formation stages that may be suited for integration with a Sabatier-based process must be developed to achieve the absolute maximum degree of loop closure. The architecture depicted by Fig. 12 incorporates a series Bosch reactor configuration that has been under development.[16]

The environmental monitoring architecture consists of an array of instruments to monitor major and trace cabin atmospheric constituents as well as combustion products and toxic chemical hazards. Major constituents are monitored using an advanced miniaturized mass spectrometer (NASA Jet Propulsion Laboratory). This mass spectrometer is a second generation design based on the successful Vehicle Cabin Atmosphere Monitor (VCAM) flight demonstration equipment. The functional backup for the mass spectrometer consists of a diode laser-based O_2 analyzer (Oxigraf Model O2) and an infrared-based CO_2 analyzer (Sable Systems Model CA-2A) operating in series. Trace constituents are monitored using a second miniature mass spectrometer integrated with a micro-electromechanical (MEMS) gas chromatograph (NASA Jet Propulsion Laboratory). Near real-time targeted toxic chemical hazard monitoring is provided using a commercial FTIR unit (Gasmet Model DX4040). An advanced optical array based on Tunable Environmental Laser Spectroscopy (TELS) technology (NASA Jet Propulsion Laboratory) is used to monitor CO and specific combustion products.

B. Future Work to Mature the Recommended Architecture

While significant progress has been realized toward an ARS and EMS architecture for exploration missions, focused developmental work is necessary to refine the architecture and address key gaps. The following discussion summarizes technical areas requiring developmental focus and investment.

1. General Operations and Integration

Throughout the ARREM Project integrated testing series, the alternative AR subsystem configurations evaluated demonstrated that an ISS-derived architecture is feasible and practical for exploration mission applications. The alternative configurations evaluated for the TCC components did not impact the core architecture's ability to achieve targeted flow rates to all areas with the exception of the instance for the M-COA inlet obtained from the chamber ventilation duct. Additional engineering will be necessary for that integration concept to be fully viable. The need to enhance the overall integration fidelity is evident in that tubing lengths and wetted materials used need to move to-

ward addressing integrated subsystem fit and form as well as materials offgassing challenges. Carbon dioxide removal performance necessary to maintain the concentration below 2 mm Hg (0.27%) was successfully demonstrated. To achieve this performance for exploration missions, a new blower design is necessary unless a future bed design can reduce pressure drop sufficiently to use heritage blower designs.

2. Carbon Dioxide Removal Function

The desiccant beds and adsorbent beds contained in the dev-CDRA ground test unit used during both the R2FD and ARREM Cycle 1 testing series have slightly different aspect ratios and, therefore, slight size differences compared to the ISS Protoflight CDRA beds used during Cycle 2 testing. Even so, the developmental CDRA equipment used during all testing series has been proven to provide valuable, comparative performance data consistent with the ISS flight CDRA equipment and has proven valuable for supporting both flight operations and technology development initiatives. The developmental CDRA equipment adsorbent beds containing either ASRT or RK-38 zeolite 5A met the required CO_2 removal capacity for exploration missions. Overall, further investigations of both the moisture removal and CO_2 removal performance is necessary to determine whether the bed sizes can be further optimized for exploration metabolic loads. As well, evaluating various candidate adsorbent media, including the media used in the ISS CDRA-4 equipment, is necessary to fully characterize durability and hydrothermal stability aspects leading to a final adsorbent media selection.

Beyond a CDRA-derived process design, developmental work on an alternative architecture derived from a combined temperature-swing adsorption-based CO_2 removal and compression process design concept must be evaluated and considered for incorporation into future process architectures.[17-18] Components and features of the combined CO_2 removal and compression process and ISS CDRA-4 with a downstream CO2 compressor and accumulator must be studied to determine where functional benefits may be realized. The potential for combining the CO_2 removal and management functions into a single, physical adsorption-based component that may eliminate the mechanical CO_2 compressor and associated accumulator tanks is attractive. Efforts to evaluate the efficacy of a thermally-regenerable amine process also must be conducted.

Emerging evidence that CO_2 concentrations aboard ISS contribute to headache sensitivities in some crewmembers as well as potentially reduce decision-making capacity may result in significantly lower maximum allowable concentration limits, conceivably below 2 mm Hg (0.27%). Therefore, the ultimate CO_2 removal assembly design must provide functional robustness capable of providing cabin CO_2 concentrations below 2 mm Hg (0.27%) to enhance crew health and performance during future crewed exploration missions.[19]

3. Trace Contaminant Control Function

The trace contaminant control architecture testing cycles investigated alternative integration approaches to eliminate blower and avionics components as well as provide broader operational flexibility and functional performance. As well, the TCC component architectures incorporated commercially available, high flow capacity activated carbon bed containment components and best-performing commercial activated carbon products as well as an advanced catalytic oxidation assembly reactor design. Advances in ammonia removal and photocatalytic oxidation of VOCs have been under consideration. Concerns exist for both photocatalytic oxidation and ammonia catalytic reduction relative to partial oxidation product and NO_x production, respectively. More work is necessary to better understand these processes relative to their utility in the trace contaminant control architecture. The commercial adsorbent and oxidation catalyst product offerings should be surveyed periodically to determine whether new advances can offer additional improvement.

4. Carbon Dioxide Reduction Function

Carbon dioxide reduction developed higher fidelity CH_4 post-processing options. Plasma methane pyrolysis, hydrogen purification, and other post-processing stages were evaluated independently and in integrated architectures with the SDU, dev-OGA, and developmental CDRA equipment. Continued developmental results from alternative CO_2 reduction technology evaluation projects, particularly those based on the Bosch process, must be evaluated and considered for incorporation into future process design concepts.[20-21]

5. Oxygen Generation Function

The ARREM Project pursued operational changes that had the greatest likelihood for reducing equipment complexity and increasing reliability. These operational changes were identified from lessons learned through ISS flight OGA operational experience. The opportunity exists to use the dev-OGA equipment to evaluate additional control software changes and procedural changes that may lead to more simple operations. Developing and demonstrating procedures to conduct cell stack polarization scans as a means to monitor cell stack health were conducted. Hardware configuration changes to further improve equipment service life to enable deep space exploration missions, including the ability to operate in low cabin pressure environments, operate with a high cell stack pressure, evaluate new cell stack membrane technologies, and address reliability challenges associated with the ISS OGA hydrogen sensor must be evaluated.

6. Environmental Monitoring Function

Developing an environmental monitoring architecture and functionally integrating it with an AR subsystem architecture is a future technical goal. The role of environmental monitoring and its relationship with the AR subsystem has been well established.[22-23] Developmental instruments consisting of commercially available FTIR spectrometry and custom-developed gas chromatography, mass spectrometry, electrochemical, and optical instruments were functionally demonstrated. Developing specific performance requirements and developing and demonstrating a complete environmental monitoring subsystem architecture that addresses major atmospheric constituent, combustion product, general VOC loading, and non-combustion chemical contamination event monitoring must be a focus for future work.

7. Autonomous Control and Process Health Monitoring

The ECLS system must become more tightly integrated with respect to core functionality, control, and equipment health monitoring to enable future exploration missions. The role of the Earth-based mission control team will change to focus on slow changes and long-term trending of baseline performance. However, under circumstances that produce changes in performance that are more rapid than the communication turnaround time with the mission control team, ECLS control will require the crew to interact with the ECLS system equipment and advanced autonomous control software. The control system must either be self-adaptable or enable the crewmembers to adapt the ECLS system to rapidly changing situations, to solve system problems, and to efficiently anticipate and schedule maintenance.[24]

The ideal function of an autonomous control system must manage the ECLS system in response to failures, functional trends, configuration changes, and environmental conditions that occur over periods in the range of tens of minutes. The control system must enable the ECLS system to operating seamlessly with no ground-based intervention under such circumstances while providing an appropriate level of automation that minimizes crew interaction as well as maintains safety-critical operations and procedures. When crew interaction is necessary, the control system must be intuitive and "crew-centered". Beyond providing functional autonomy and an appropriate automation level, additional aspects of autonomous control and process health monitoring include command and data handling (C&DH), software development and testing to achieve maturity comparable to core ECLS system process technologies, hardware-software complexity, and crew interfaces.[25]

8. Equipment Fit and Form

The components and test articles used during the ARREM Project spanned a range of maturity from developmental through ISS flight-like functional mockup based on flight hardware drawings. Integration between components and assemblies was functional only. Results obtained during the ARREM Project have indicated the potential for reducing the equipment size in nearly all functional areas. Addressing equipment component size and integration relative to overall fit and form must be accomplished to fully realize the potential for performance benefits, particularly relating to mass and volume reduction. To accomplish this, detailed process and instrumentation diagrams for the entire equipment architecture must be developed and component size characteristics determined. From this information, detailed computer-aided design solid models must be prepared to facilitate fit and form studies for the core AR system architecture and its extension to missions requiring a high degree of mass closure.

VI. Conclusion

An AR subsystem architecture that builds on the framework established by the ISS AR process design has been developed and demonstrated. Demonstration results show that the physical architecture is feasible and areas have been identified to improve reliability while reducing overall mass, volume, and complexity.

The core subsystem architecture's performance meets or exceeds the performance attained by the ISS AR subsystem. Mass reduction of at least 35 kg with accompanying volume reduction compared to the ISS AR subsystem were demonstrated by integrating the trace contaminant control components in a different manner and modifying O_2 generation assembly operational parameters. Additional savings beyond the AR subsystem may be possible through reducing the trace contaminant load presented to humidity condensate which can reduce logistics demands for the water processing subsystem. Incorporating results of detailed engineering analysis of the four-bed CO_2 removal process architecture to size the equipment for a four crewmember metabolic load as well as incorporating contemporary adsorbent media and adjusting process conditions will provide additional mass and volume reduction compared to the SOA basis. Additional work is necessary in this area to quantify the potential mass and volume reduction.

Opportunity exists to demonstrate a higher degree of resource mass closure by incorporating CH_4 post-processing techniques. Further reliability for the O_2 generation equipment architecture is possible by incorporating contemporary cell stack membrane materials and incorporating operational lessons learned from ISS flight experience. Continued work on O_2 loop closure and contemporary electrolytic cell stack designs is required.

Appendix

Single Crewmember Basis for Table 3.

COMPOUND	ACTIVITY	RATE (kg/CM-h)
H_2O	Sleep	0.0378
	Normal	0.0706
	Exercise	0.629
	Post Exercise	0.281
CO_2	Sleep	0.027
	Normal/Post Ex.	0.047
	Exercise	0.3
O_2	Sleep	0.022
	Normal/Post Ex.	0.038
	Exercise	0.24

Human Integration Design Handbook, NASA SP-2010-3407, pp. 337-339.

Acknowledgments

The authors thank the NASA Advanced Exploration Program for its support and the Jacobs Engineering ECLSS test team for test setup and execution.

References

[1]Perry, J., Knox, J., Parrish, K., Roman, M., Jan, D., and Abney, M., "Integrated Atmosphere Resource Recovery and Environmental Monitoring Technology Demonstration for Deep Space Exploration," AIAA 2012-3585. *AIAA 42nd International Conference on Environmental Systems*, San Diego, California, 2012.

[2]Roman, M., Perry, J., and Jan, D., "Design, Development, Test, and Evaluation of Atmosphere Revitalization and Environmental Monitoring Systems for Long Duration Missions," AIAA 2012-5120, *AIAA Space and Astronautics Forum and Exposition*, Pasadena, California, 2012.

[3]Howard, D., Perry, J., and Roman, M., "Lessons Learned from the Development and Implementation of the Atmosphere Resource Recovery and Environmental Monitoring Project," *AIAA Space 2014 Conference and Exposition*, Pasadena, California, August 2014.

[4]Hodgson, E., Converse, D., Duggan, M., and Gentry, G. "Flexible Path Environmental Control and Life Support Technology—Possible First Steps to Move Beyond LEO," AIAA-2012-3443, *AIAA 42nd International Conference on Environmental Systems*, San Diego, CA, 2012.

[5]Perry, J., Abney, M., Frederick, K., Greenwood, Z., Kayatin, M., Newton, R., Parrish, K., Takada, K., Miller, L., Scott, J., and Stanley, C., "Functional Performance of an Enabling Atmosphere Revitalization Subsystem Architecture for Deep Space Exploration Missions," AIAA 2013-3421, *AIAA 43rd International Conference on Environmental Systems*, Vail, Colorado, 2013.

[6]Perry, J. L., Tatara, J.D., Performance of Off-the-Shelf Technologies for Spacecraft Cabin Atmospheric Major Constituent Monitoring, NASA/TM-2004-213392.

[7]Human Integration Design Handbook, NASA SP-2010-3407, pp. 337-339.

[8]Coleman, H. W. and Steele, W. G., *Experimentation and Uncertainty Analysis for Engineers*, John Wiley & Sons, Inc., 1989, pp. 7-14, 76-118.

[9]Takada, K., Ghariani, A. E., and Van Keuren, S., "Advancing the Oxygen Generator Assembly Design to Increase Reliability and Reduce Costs for Future Long Duration Missions," ICES-2015-115, *45th International Conference on Environmental Systems*, Bellevue, Washington, 2015.

[10]Woods, S., "OGA Test Bed Operation with Nitrogen Purge Disabled," Hydrogen Hazards Memorandum HMEM.013, White Sands Test Facility Hydrogen Group, January 2014.

[11]Mulloth, L. M., Perry, J. L., and LeVan, D. "Integrated System Design for Air Revitalization in Next Generation Crewed Spacecraft," SAE 2004-01-2373, *34th International Conference on Environmental Systems*, Colorado Springs, CO, 2004.

[12]Vilekar, S. A., Hawley, K., Junaedi, C., Roychoudhury, S., Perry, J. L., and Kayatin, M. J., "Microlith®-based Catalytic Reactor for Air Quality and Trace Contaminant Control Applications," ICES-2015-278, *45th International Conference on Environmental Systems*, Bellevue, Washington, 2015.

[13]J. Knox, H. Gauto, R. Gostowski, D. Trinh, D. Watson, J. Hogan, J. Thomas, and E. King, "Development of Carbon Dioxide Removal Systems for Advanced Exploration Systems 2012-2013," AIAA 2013-3422. *AIAA 43rd International Conference on Environmental Systems,* Vail, Colorado, 2013, pp. 6-9.

[14]J. Hogan, B. Luna, L. Mulloth, M. Varghese, B. Koss, G. Palmer, P. Linggi, J. Melton, and Z. Lu, "The Low-Power CO_2 Removal and Compression System: Design Advances and Development Status," AIAA 2012-3587 *AIAA 42nd International Conference on Environmental Systems,* San Diego, California, 2012.

[15]Abney, M. B., Greenwood, Z., Miller, L. A., Alvarez, G., Iannantuono, M., and Jones, K., "Methane Post-Processor Development to Increase Oxygen Recovery beyond State-of-the-Art Carbon Dioxide Reduction," AIAA 2013-3513, *AIAA 43rd International Conference on Environmental Systems,* Vail, Colorado, 2013.

[16]Abney, M., Mansell, J., Long, D., Evans, C., Swickrath, M., Miller, L., Thomas, J. "Series Bosch System Development," AIAA-2012-3554, *AIAA 42nd International Conference on Environmental Systems,* San Diego, CA, 2012

[17]Varghese, M., Mulloth, L., Luna, B., and Hogan, J. "Development Status of a Low-Power CO_2 Removal and Compression System for Closed-Loop Air Revitalization", AIAA-2010-6060, *AIAA 40th International Conference on Environmental Systems,* Barcelona, Spain, 2010.

[18]Hogan, J., Luna, B., Mulloth, L., Varghese, M., Koss, B., Palmer, G., Linggi, P., Melton, J., and Lu, Z. "The Low-Power CO_2 Removal and Compression System: Design Advances and Developmental Status," AIAA-2012-3587, *AIAA 42nd International Conference on Environmental Systems,* San Diego, CA, 2012.

[19]James, J., and Matty, C. "Crew Health and Performance Improvements with Reduced Carbon Dioxide Levels and the Resource Impact to Accomplish Those Reductions," AIAA-2011-5047, *AIAA 41st International Conference on Environmental Systems,* Portland, OR, 2011.

[20]Wheeler, R., Hadley, N., Dahl, R., Abney, M., Greenwood, Z., Miller, L., Medlen, A. "Advanced PPA Reactor and Process Development," AIAA-2012-3553, *AIAA 42nd International Conference on Environmental Systems,* San Diego, CA, 2012.

[21]Abney, M., Mansell, J., Long, D., Evans, C., Swickrath, M., Miller, L., Thomas, J. "Series Bosch System Development," AIAA-2012-3554, *AIAA 42nd International Conference on Environmental Systems,* San Diego, CA, 2012.

[22]Jan, D. "Environmental Monitoring as Part of Life Support for the Crew Habitat for Lunar and Mars Missions," AIAA-2010-6092, *AIAA 40th International Conference on Environmental Systems,* Barcelona, Spain, 2010.

[23]Jan, D., and Newton, R. "Environmental Monitoring as Part of Life Support: Preparing for Deep Space Missions," AIAA-2012-3433, *AIAA 42nd International Conference on Environmental Systems,* San Diego, CA, 2012.

[24]"Charter for Advanced System Integration and Control for Life Support", Workshop on Advanced System Integration and Control for Life Support, Monterey, California, August 2003.

[25]"Advanced Life Support Systems," Workshop on Advanced System Integration and Control for Life Support, Monterey, California, August 2003.